BCKDK Promotes EOC Proliferation and Migration By Activating The MEK/ERK Signaling Pathway

Huashun Li
: First People's Hospital of Foshan
Dongyang Yu
Wuhan Children's Hospital
Lianbing Li
Chongqing Population and Family Planning Science and Technology Research Institute
Juanjuan Xiao
The Affiliated Hospital of Guilin Medical University
Yijian Zhu
Chongqing Population and Family Planning Science and Technology Research Institute
Yi Liu
Chongqing Population and Family Planning Science and Technology Research Institute
Li Mu
Chongqing Population and Family Planning Science and Technology Research Institute
Yafei Tian
Chongqing Population and Family Planning Science and Technology Research Institute
Linbo Chen
Chongqing Population and Family Planning Science and Technology Research Institute
Feng Zhu
The Affiliated Hospital of Guilin Medical University
Qiuhong Duan
Huazhong University of Science and Technology
Peipei Xue (xuepeipei@alumni.hust.edu.cn)
Chongqing Population and Family Planning Science and Technology Research Institute https://orcid.org/0000-0002-2071-4815

Primary research

Keywords: EOC, BCKDK, proliferation, migration, MEK

Posted Date: April 12th, 2021

DOI: https://doi.org/10.21203/rs.3.rs-375348/v1

Abstract

Background: Ovarian cancer is the most fatal gynecologic cancer, and epithelial ovarian cancer (EOC) is the most common type. The branched-chain α-keto acid dehydrogenase kinase (BCKDK) plays an important role in many serious human diseases, including cancers. Its function in promoting cell proliferation and migration has been reported in various cancers. However, the biological role of BCKDK and its molecular mechanisms underlying EOC initiation and progression are unclear.

Methods: First, the expression level of BCKDK in EOC cell lines or tissues was determined using tissue microarray (TMA)-based immunohistochemistry or western blotting. Then, growth curve analysis, anchorage-independent cell transformation assays, wound healing assays, cell migration assays, and tumor xenografts were used to test whether BCKDK could promote cell transformation or metastasis. Finally, the signaling pathways involved in this process were investigated by western blotting or immunoprecipitation.

Results: We found that the expression of BCKDK was upregulated in EOC tissues and that high expression of BCKDK was correlated with an advanced pathological grade in patients. The ectopic overexpression of BCKDK promoted the proliferation and migration of EOC cells, and the knockdown of BCKDK with shRNAs inhibited the proliferation and migration of EOC *ex vivo* and *in vivo*. Moreover, BCKDK promoted EOC proliferation and migration by targeting MEK.

Conclusions: Our results demonstrate that BCKDK promotes EOC proliferation and migration by activating the MEK/ERK signaling pathway. Targeting the BCKDK-MEK axis may provide a new therapeutic strategy for treating patients with EOC.

Background

Ovarian cancer (OC) is the second most common malignancy after breast cancer in women over the age of 40 [1]. However, it is the most fatal gynecologic cancer [2]. Because it remains a challenge to diagnose early. There are three main types of ovarian cancer: epithelial, germ cell, and sex-cord stromal. Epithelial ovarian cancer (EOC) is the most common type, comprising about 95% of all ovarian cancers [2, 3]. About 75% of patients are diagnosed at an advanced stage because of the asymptomatic nature of EOC.

Endometriosis has been linked to some EOC. However, no evidence shows that removal of endometriosis lesions will decrease a woman's chances of developing OC [4]. The biomarker, such as serum cancer antigen 125 (CA125) or human epididymis protein 4, combined with transvaginal sonography was tested for some OC. A randomized controlled trial of over 200000 women assessing annual multimodal screening with CA125, did not identify significant mortality reduction when the risk for ovarian cancer algorithm was used, versus annual transvaginal ultrasound screening, versus no screening [5]. Therefore, over the last 30 years, mortality rates from OC, including EOC, have narrowly dropped [1, 6]. On the other hand, PARP1 inhibitors (Niraparib, Olaparib and Rucaparib) maintenance therapy was recently shown to substantially improve progression-free survival in ovarian cancer patients [7–10]. However, not all patients respond to PARP inhibitor therapy, either due to intrinsic or acquired resistance to PARP inhibitors [10–12]. Therefore, the development of alternative synthetic lethality targets is urgently needed in EOC.

Branched-chain α-keto acid dehydrogenase kinase (BCKDK) located in the mitochondrial matrix, belonging to pyruvate dehydrogenase kinases (PDKs) family [13], which promoted the proliferation and metastasis of various tumors and was considered to be a strong therapeutic target for preventing tumors development [14–19]. Dysfunction of BCKDK was closely related to various human diseases, especially maple syrup urine disease. Bravo-Alonso and Oyarzabal found the excessive function of BCKDK resulted in maple syrup urine disease [20–22]. As diabetics had increased susceptibility to ovarian cancer, always divided into late stages when the first diagnosis and had a poor prognosis [23]. Over-expression of BCKDK resulted in branched-chain amino acid (BCAA) increase, elevated plasma levels of BCAA were associated with a greater than 2-fold increased risk of future pancreatic cancer diagnosis [24]. Leu promoted adipose tissue protein synthesis through mTOR pathway [25], and then adipocytes promoted ovarian cancer metastasis and provided energy for rapid tumor growth [26]. BCKDK promoted colorectal cancer and hepatocellular carcinoma metastasis and proliferation via the ERK signaling pathway [27–29]. Furthermore, BCKDK was highly expressed in DOX-induced ovarian cancer drug-resistant cell lines, and its expression level was twice as high as that of sensitive one [30]. Inhibition of BCKDK increased the sensitivity of ovarian cancer cells to paclitaxel [31]. We can't help but wonder if BCKDK could promote ovarian cancer proliferation and metastasis? Which pathways worked in this process?

In this study, We showed that the BCKDK had a higher expression in EOC patients versus normal tissues. The high expression of BCKDK was correlated with the advanced pathological grade for patients. Overexpression of BCKDK increased the clone formation and migration ability of SKOV3 and OVCAR3 cells *ex vivo.* Knockdown of BCKDK inhibited EOC tumor progression *ex vivo* and *in vivo*. And we identified BCKDK as an upstream kinase of MEK, which up-regulated MEK/ERK signaling by interacting with MEK. The above results suggest that BCKDK may promote EOC proliferation and migration through enhancing the MEK/ERK signaling pathway.

Methods

Plasmids, shRNA, antibodies, and other reagents

The plasmid of pCMV-C-Flag (catalog: D2632) was purchased from Beyotime Biotechnology (Shanghai, China). The plasmids of pDONR223-BCKDK (catalog: 23794) was purchased from Addgene (Cambridge, MA, USA). The plasmids of pCMV-BCKDK-Flag and pLKO.1-shBCKDK were constructed by our laboratories. 5 sequences were designed to knock down BCKDK, and the sequences are: 1. 5'-CCGGGATCTGATCATCAGGATCTCACTCGAGTGAGATCCTGATGATCAGATCTTTTTG-3'; 2. 5'-CCGGTCAGGACCCATGCACGGCTTTCTCGAGAAAGCC

GTGCATGGGTCCTGATTTTTG-3'; 3. 5'-CCGGCGTCCGCTACTTCTTGGACA

ACTCGAGTTGTCCAAGAAGTAGCGGACGTTTTTG-3'; 4. 5'-CCGGACGCTG

ACTTCGAGGCTTGGACTCGAGTCCAAGCCTCGAAGTCAGCGTTTTTTG-3'; 5.5'-CCGGCCAGCACCAGTTCCGTCATTCCTCGAGGAATGACGGAACTGGTGCTGGTTTTTG-3'. A mock shRNA with a sequence lacking significant homology to the human genome database was used as the mock shRNA. The sequence was: 5'-CCGGCCTAAGGTTAAGTCGCCCTCGCTCGAGCGAGGGCGACTTAACCTTAGGTTTTTG-3'. The sense

and anti-sense oligonucleotides were synthesized, annealed and cloned into the pLKO.1-TRC cloning vector at the *EcoRI* and *AgeI* sites as described by the manufacturer [32].

Anti-p-MEK1/2 (ser221) (catalog: 2338), t-MEK (catalog: 8727), phospho-p44/42MAPK (Erk1/2) (T202/Y204) (D13.14.4E) (catalog: 4370), and t-ERK (catalog: 4695) antibodies were purchased from Cell Signaling Technology (Danvers, MA, USA). Anti-mouse BCKDK antibody (catalog: sc-374425) and Anti-β-actin antibody (catalog: sc-130656) were purchased from Santa Cruz Technology, Inc (Santa Cruz, CA, USA). HRP-conjugated anti-rabbit (catalog: E030120) antibody and HRP-conjugated anti-mouse antibody (catalog: E030110) were purchased from EarthOx Life Sciences (San Francisco, CA, USA). Anti-Flag antibody (catalog: F1804, catalog: F7425) was purchased from Sigma-Aldrich (St. Louis, MO, USA). G418 (catalog: A1720) and puromycin were purchased from Sigma-Aldrich (St. Louis, MO, USA) and used for setting up stable cell lines. Simple-Fect (catalog: Profect-01) was purchased from Signaling Dawn Biotech (Wuhan, Hubei, China) for transfection.

Cell Culture

The human epithelial ovarian cancer cell lines (HO8910, HO8910-PM, SW626, SKOV3 and OVCAR3) and the normal cell lines (IOSE80 and HEK293T) were purchased from American Type Culture Collection (ATCC; Manassas, VA, USA). IOSE80 and HEK293T cells were cultured in Dulbecco's Modified Eagle's Medium (Gibco, Gaithersburg, MD, USA) supplemented with 10% fetal bovine serum (FBS) (Gibco, Gaithersburg, MD, USA) and 2 mmol/L glutamine (Gibco, Gaithersburg, MD, USA). HO8910 and HO8910-PM cells were cultured in RPMI-1640 (Gibco) supplemented with 10% FBS and 2 mmol/L glutamine. SKOV3 cells were cultured in McCoy's 5A (Gibco) supplemented with 10% FBS and 2 mmol/L glutamine. OVCAR3 were cultured in RPMI-1640 (Gibco) supplemented with 20% FBS and 2 mmol/L glutamine. All cells were grown in 5% CO_2 with saturated humidity at 37°C.

Western blot

Cells ($0.8\text{-}2\times10^6$) were cultured in 10 cm diameter dishes to 70–80% confluence, and then starved no serum for 24h. Then the cells were treated with 40 ng/mL epidermal growth factor (EGF) (R&D catalog: 236-EG-200) for 15min. EGF is a well-known tumor promotion agent used to study malignant cell transformation in animal and cell models of cancer [33]. After this, cells were washed twice in PBS before being lysed in RIPA buffer (Coolaber, China). Then, samples were sonicated in 15 seconds intervals three times, and insoluble debris was removed by centrifugation at 13000 rpm for 15 min. Protein content was determined by BCA method (Coolaber, China). 30–120 μg of protein was separated by 10% SDS-PAGE and visualized by chemiluminescence (BIO-RAD, USA) in triplicate.

Growth curve analysis

2×10^5 cells were plated in each dish and counted at different times in triplicate, using a hemacytometer to generate a growth curve.

Anchorage-independent cell transformation assay

Different cell lines (8×10^3/well) were seeded in 6-well plates. The cells were then cultured in 1 mL of Agar (Sigma-Aldrich Corp.) containing 10% FBS, 0.33% BME (Eagle basal medium, Sigma-Aldrich Corp.), 25 μg/mL gentamicin and 2 mM L-glutamine, with an additional 3ml of 2 mM L-glutamine, 0.5% BME agar containing 10% FBS and 25 μg/mL gentamicin being below. Then the cells were maintained in a 37°C, 5% CO_2 incubator for 7–14 days and the colonies were observed and assessed by microscopy.

Tumor xenografts and the tissue microarray (TMA) assay

Female athymic Balb/c nude mice (4–6-week-old) were purchased from Chongqing Tengxin Beer Experimental Animal Sales CO, LTD (Chongqing, China). Mice were kept in specific pathogen-free conditions according to the National Guidelines for Animal Usage in Research (set by the Chinese government) at the Chongqing Population and Family Planning Science and Technology Research Institute. Mice were divided and randomized into three groups. Each of the different cell lines (3×10^6 in 200 μl PBS) was injected subcutaneously into the right flank. The tumor volumes were measured every three day and were calculated with the formula: V = 0.52 (length ×width × height). The tumor tissues were prepared with paraffin sections after fixation with formalin, and then stained with hematoxylin and eosin (H&E).

The TMA underwent EOC (catalog: FOV 1006) were purchased from Xi'an Elena Bio Co., Ltd. Samples were obtained with informed consent. The TMA was stained with anti-BCKDK. The immuno-scores were calculated following the Remmele score method (Regitnig et al., 2002), and the scores greater than 2 were used as positive group, the others were used as negative group.

Wound healing assay

The wound healing assays were applied to determine the migration ability of cells. 2×10^5 cells were cultured in a six-well plate until 80–90% confluence and then carefully scratched with a 10 μL pipette tip. After washing three times with 1×PBS to remove detached cells, images in 10 different wound fields were captured at respective time points (0 h and 48 h) to evaluate the migration of cells.

Cell migration assay (trans-well assay)

Chambers (catalog: 3422, 8μm pore, Corning, NY, USA) were used to investigate migration ability of cells. 1×10^5 cells suspended in 150 μL serum-free medium were seeded onto the upper chamber of 24-well plates, and 700 μL of medium with 10% FBS was added to the lower chamber. 48 h later, the medium was removed from the upper chamber. The non-migrating cells on the upper side of the chamber were removed thoroughly with a clean cotton swab. Then cells on the bottom side of the membrane were fixed with 4% paraformaldehyde for 30 min, then stained with 0.1% of crystal violet (Sangon Biotech) for 15 min. Finally, the stained cells were counted by microscopy. Results represent the average number of cells in three fields per membrane in triplicate inserts.

Immunoprecipitation

HO8910-PM were seeded in 10cm dishes for 24h. Then, cells were harvested in IP buffer (150mM NaCl, 50mM tris-HCl pH 7.4, 1% NP40, 1mM DTT and 1mM EDTA). 2mg proteins were subjected to immunoprecipitation following the manufacturer's instructions. (Http://www.scbt.com/protocols.html?protocol=immunop

recipitation). The mouse source antibody was used for IP and the rabbit source antibody was used for western blotting.

Statistical analysis

All quantitative data in the present study were performed at least in triplicate. The results are expressed as the mean ± standard deviation. A two-tailed ANOVA or Student's t-test was used to evaluate the data. Correlation data were determined by using Pearson correlation coefficients. And $P< 0.05$ was considered significant (*$p< 0.05$, ** $p< 0.01$, ***$p< 0.001$).

Results

BCKDK over-expression is associated with advanced pathological grade in EOC patients.

First, BCKDK expression level was analyzed in 5 EOC cell lines and 1 normal ovarian epithelial cell line (Fig. 1a). The results showed that BCKDK was highly expressed in HO8910-PM and SW626 cells, moderately expressed in HO8910 cells, and poorly expressed in SKOV3 and OVCAR3 cells. The BCKDK level of normal IOSE80 cells was the lowest. Then, the expression level of BCKDK was analyzed in EOC tissue and corresponding tumor adjacent tissue samples. The results indicated that expression level of BCKDK was higher in cancer tissue than adjacent tissue (Fig. 1b, 1c), and is correlated with advanced pathological grade for patients(Fig. 1e). Detailed information on patients is shown in Fig. 1d.

BCKDK promotes EOC cell proliferation

To test whether BCKDK can promote cell transformation, BCKDK was overexpressed in SKOV3 and OVCAR3 cells which poorly expressed BCKDK. SKOV3 and OVCAR3 stable cell lines that overexpressed the pCMV-c-Flag or pCMV-BCKDK-Flag were generated, and the growth curves of SKOV3-Mock and SKOV3-BCKDK cells, or OVCAR3-Mock and OVCAR3-BCKDK cells were compared. The results showed that SKOV3-BCKDK cells grew faster than SKOV3-Mock cells (Fig. 2a, inner session indicating BCKDK overexpression). Next, the anchorage-independent growth of SKOV3-Mock or SKOV3-BCKDK was compared, and the result indicated that the number of colonies in SKOV3-BCKDK cell cultures was much more than that in SKOV3-Mock cell cultures (Fig. 2c left panel). The corresponding statistical significance is shown in the right panel of Fig. 2c. Similar results were observed in the cultures of OVCAR3-Mock or OVCAR3-BCKDK stable cells (Fig. 2b, 2d). These results indicate that BCKDK promotes cell proliferation.

BCKDK promotes EOC cell migration

Since BCKDK is tightly linked to tumor migration in colorectal caner [28], we wondered whether BCKDK also regulated EOC metastasis. To test this speculation, wound healing cell migration and transwell assays were performed to investigate the effects of BCKDK on the migration of SKOV3 and OVCAR3 cells. The outcomes are shown in Fig. 3a demonstrating that BCKDK could accelerate the migration and invasion of EOC cells. These results suggest that BCKDK influences EOC metastasis. Wound healing assays indicated that over-expression of BCKDK accelerate the migration of SKOV3 and OVCAR3 cells (Fig. 3a, 3b). In addition, transwell assays showed that over-expression of BCKDK enhanced the invasive ability of SKOV3 and OVCAR3 cells (Fig. 3c, 3d).

Knockdown of BCKDK attenuates EOC tumor properties

To verify this idea further, BCKDK was knocked down in HO8910-PM EOC cells to generate the stable shBCKDK cell lines and the stable shMock cell lines (HO8910-PM-shBCKDK, HO8910-PM-shMock). As shown in Fig. 4a inner session of left panel by the result of Western blot, BCKDK was knocked down by shRNA sequence for lines 2 and 4. Growth curves of HO8910-PM-shMock, -shBCKDK2, or -shBCKDK4 cells were tested, and the results demonstrated that HO8910-PM-shBCKDK cells grew dramatically slower than HO8910-PM-shMock cells (Fig. 4a). Next, the anchorage-independent growth of the HO8910-PM-shMock or HO8910-PM-shBCKDK cell lines was evaluated, and the results indicated that the number of colonies in HO8910-PM-shBCKDK cell cultures was much less than in HO8910-PM-shMock cell cultures (Fig. 4b). And wound healing assays and transwell assays of the HO8910-PM-shMock or HO8910-PM-shBCKDK cell lines were also performed, and the results indicated that knockdown of BCKDK attenuated the migration and invasion of HO8910-PM cells (Fig. 4c, 4d). Therefore, these results indicated that knockdown of BCKDK in ovarian tumor cells inhibited tumorigenesis and metastasis *ex vivo*. Then, tumor

xenograft assays were preformed in female athymic Balb/c nude mice. We injected HO8910-PM-shMock, -shBCKDK2, or -shBCKDK4 cells (3×10^6) subcutaneously into the right flank, with tumor size assessed over time. Tumors in HO8910-PM-shMock-inoculated mice grew to a much larger size compared to those in HO8910-PM-shBCKDK-inoculated mice (Fig. 5a, 5b). The tumor growth curve was shown in Fig. 5c. The final weight of tumor was shown in Fig. 5d. And the tumor tissues dissected from the xenografts in the study were stained with hematoxylin & eosin (H&E) to confirm these tissues belong to tumor tissues (Fig. 5e). These data demonstrated that blocking BCKDK expression in EOC cells significantly reduces their tumorigenic properties *ex vivo* and *in vivo*, and further confirmed that BCKDK promotes cell proliferation and migration.

BCKDK promotes tumor properties through up-regulating the MEK-ERK signaling pathway

We confirmed that BCKDK promoted cell proliferation and migration *ex vivo* and *in vivo*. Next, we wanted to know which signaling pathway was involved in this process. BCKDK promotes carcinogenesis has been reported in coloreactal cancer and hepatocellular carcinoma [27, 29]. Therefore, p-MEK1/2 (ser221) and p-ERK1/2 (T202/Y204) levels were tested in OVCAR3 and SKOV3 BCKDK stable cell lines, and the results indicated that the level of p-MEK and p-ERK were up-regulated when BCKDK was overexpressed (Fig. 6a, 6b). These results suggest that BCKDK promotes EOC through up-regulating MEK-ERK activity. Next, the level of p-MEK and p-ERK were tested in the HO8910-PM-shBCKDK cell lines. Both p-MEK and p-ERK were decreased significantly when BCKDK was knocked down in HO8910-PM cell lines (Fig. 6c). Next, the expression level of p-MEK1/2 (Ser221), p-ERK1/2(T202/Y204), and BCKDK were detected in dissected tumor tissues by Western Blotting. The results confirmed that the level of p-MEK1/2 (Ser221), p-ERK1/2(T202/Y204), and BCKDK were higher in the tumor tissue of HO8910-PM-shMock mice than in the tumor tissue of HO8910-PM-shBCKDK mice (Fig. 6d). These data confirmed that BCKDK promoted tumor properties through up-regulating the MEK-ERK signaling pathway.

BCKDK interacts with MEK

We found BCKDK directly interacted with MEK in colerectal cancer cells in before research [27]. Therefore, We wounder whether BCKDK also interacts with MEK in EOC cells? Then, BCKDK was immunoprecipitated from HO8910-PM cells, and was detected by Western blotting with a MEK antibody. The results indicated that BCKDK could co-immunoprecipitates with MEK in HO8910-PM cells (Fig. 6e).

Taken together, our study indicates that BCKDK promotes EOC proliferation and migration through enhancing the MEK/ERK signaling pathway.

Discussion

OC is one of the most lethal cancers among women. As OC usually develops without well-defined clinical symptoms, it is diagnosed mostly in advanced stages with poor five-year survival rates of 15–45% [34]. On the other hand, FIGO stage I OC is associated with a 90% or higher survival rate. To improve the diagnostic procedures and identify OC patients in early stages of the disease, various serum markers have been developed and used. CA125 was first reported as a tumor marker to detect ovarian tumors in the 1980s [35]. However, the sensitivity and specificity of these markers are not high [36, 37]. Therefore, the development of specific serum markers for screening without internal examinations is urgently needed, particularly for patients with ovarian cancer, who typically do not

present any symptoms until an advanced stage. In addition, over the last 30 years, mortality rates from OC, including EOC, have slightly dropped [6, 38]. The development of alternative synthetic lethal targets and diagnostic biomarkers is urgently needed.

The amino acid profile has been identified as an effective diagnostic tool in different cancers previously [39–42], and some amino acids are associated with OC [43–46], for example, leu [47]. Branched-chain amino acid (BCAA) catabolism is closely related to tumors. The loss of BCAA catabolism promotes tumor development and growth [48, 49]. The suppression of BCAA catabolic enzyme expression led to BCAA accumulation in tumors but not in regenerating liver tissues [48]. Current research focuses on BCAT1 or BCAT2, which works in the first step of BCAA catabolism, while there are relatively few studies on BCKDK, which is a key negative regulatory enzyme in BCAA catabolism [50–53]. Despite this, studies have shown that the overexpression of BCKDK promotes the growth and metastasis of various tumors [27–29]. In this study, we determined that BCKDK promoted the proliferation and metastasis of EOC, and BCKDK was expressed at higher levels in EOC tissues than in adjacent normal tissues (Fig. 1b) and is correlated with advanced pathological grade for patients(Fig. 1e). This suggests that BCKDK could be another potential biomarker for the treatment of EOC. Inhibitors targeting BCKDK will be examined in future research.

Current research of BCAA catabolism worked in tumors focused on BCAT. As the BCAT reaction is reversible and near equilibrium, its direction should respond to changes in concentrations of BCAA and BCKAs, and availability of the donors and acceptors of nitrogen, to some extent, the conclusion was opposite in different researches. For example, some studies confirmed that the high expression of BCAT promoted the transfer of the BCAA amino group to α-ketoglutarate (α-KG) to form glutamate and the corresponding branched-chain keto acids (BCKAs). The BCAA catabolism was increasing, then the BCA-CoA entering into tricarboxylic acid cycle that provided energy for tumor cells proliferation and growth [53, 54]. The other studies verified that the catabolism of BCAA in tumor cells was decreasing, and the high expression of BCAT promoted the conversion of BCKAs to BCAA and α-KG, and then providing essential nutrients and energy for cancer growth [48–49, 55]. Our research supports the second. The overexpression of BCKDK inhibits the conversion of BCKAs to BCA-CoA, which leads to the accumulation of BCKAs. Furthermore, the accumulation of BCKAs inhibits BCAA catabolism. Therefore, BCKAs are converted into BCAAs again through amination with the BCAT enzyme. In addition, there are studies showing that BCKDK and PPM1K make up a ChREBP-regulated node that integrates BCAA and lipid metabolism and promotes BCAAs as a material for fat synthesis for fat cells, which provide energy for tumor growth [56]. It has been proven that leu was increased in OC [47]. Other studies also found that the overexpression of BCAT promoted OC proliferation [51–53]. Therefore, our research gave a further understand of BCAA catabolism worked in the ovarian cancer. While, how BCKDK coordinated with BCAT to balance the BCAA metabolism? And whether they could directly regulate each other was still unclear.

Furthermore, to confirm the function of BCKDK in EOC, BCKDK was overexpressed in SKOV3 and OVCAR3 cells which poorly expressed BCKDK. BCKDK gain significantly promoted the proliferation and migration *ex vivo*, whereas knocked down the expression of BCKDK in HO8910-PM EOC cells reduced the proliferation and migration *ex vivo* and inhibited the tumor growth *in vivo*. Hence, these data supported the tumor-promoting function of BCKDK in EOC. These results were also consistent with previous findings demonstrating that BCKDK is a key regulator of cell proliferation and metastasis in colorectal cancer and hepatocellular carcinoma [27–29]. Moreover, BCKDK promotes EOC proliferation and migration by activating the MEK/ERK signaling pathway. In agreement with our previous study, our previous study demonstrated that BCKDK promoted colorectal cancer proliferation by targetting the MEK1 [27]. Another previous study also verified that BCKDK promoted hepatocellular cancer proliferation by

MEK/ERK signaling pathway [29]. To our knowledge, this study was the first to report the ectopic expression of BCKDK in EOC, and uncovered the mechanism that BCKDK regulates EOC proliferation and migration by MEK/ERK signaling pathway.

Other studies also showed that BCKDK was closely related to lipid metabolism, which was upregulated by APN [55]. In addition, BCKDK promoted tumor growth and metastasis by interacting with SRC or mTOR in colon cancer or hepatic carcinoma (Fig. 7) [28, 29]. Therefore, in addition to the MEK-ERK pathway, whether the APN, SRC, or mTOR signaling pathways are also involved in this process still needs further examination. In addition, the drug resistance of ovarian cancer is a thorny issue, and and the mitochondria are closely related to apoptosis and autophagy-induced drug resistance [58–60]. As BCKDK is located in the mitochondria, and related to drug resistance in ovarian cancer [30–31]. What is the relevant mechanism? Many questions need to be addressed in the future. Due to the limited samples in this study, future studies need to expand the number of clinical samples and collect more clinical information.

Conclusions

These findings indicated that the expression of BCKDK was upregulated in EOC tissues and that high expression of BCKDK was correlated with advanced pathological grade in patients. BCKDK promoted EOC proliferation and migration by targeting MEK. Targeting the BCKDK-MEK axis may provide a new therapeutic strategy for treating patients with EOC.

Abbreviations

OC: Ovarian cancer; EOC: epithelial ovarian cancer; BCKDK: branched-chain α-keto acid dehydrogenase kinase; CA125: cancer antigen 125; PDKs: pyruvate dehydrogenase kinases; BCAA: branched-chain amino acid; ERK: extracellular signal-regulated kinase; EGF: epidermal growth factor; TMA: tissue microarray; BME: Eagle basal medium; H&E: hematoxylin and eosin; α-KG: α-ketoglutarate; BCKAs: branched-chain keto acids.

Declarations

Ethics approval and consent to participate

The study got approved by the Ethics Committee of the Chongqing Population and Family Planning Science and Technology Research Institute. (Ethic approval number:

2019D001).

Consent for publication

All authors involved in the authorship are consent for publication in the current form.

Availability of data and materials

Not applicable.

Competing interests

The authors declare that they have no competing interests.

Funding

This project was supported by the Key Program of the National Natural Science Foundation of China (No. 81630087), and the National Natural Science Foundation of China (No. 81902849), and the Chongqing Population and Family Planning Science and Technology Research Institute (No. cstc2017jxjl30002, No. cstc2017jxjl130027, No. cstc2019jxjl130001), and the Natural Science Foundation of Chongqing (No. cstc2019jcyj-msxmX0825), and the Hubei Province Health and Family Planning Scientific Research Project (No. WJ2019M109).

Authors' contributions

Dongyang Yu, Yi Liu, and Yafei Tian were involved in the acquisition of experimental data. Huashun Li performed the tissue microarray analysis. Juanjuan Xiao analyzed the clinical data. Li Mu and Yijian Zhu housed and maintained the mice. Lianbing Li and Linbo Chen provided advice on the manuscript. Feng Zhu, Qiuhong Duan and Peipei Xue designed the study, analyzed the data and drafted the manuscript.

Acknowledgements

We sincerely appreciate all lab members.

References

1. Torre LA, Trabert B, DeSantis CE, Miller KD, Samimi G, Runowicz CD, Gaudet MM, Jemal A, Siegel RL. Ovarian cancer statistics, 2018. CA Cancer J Clin. 2018; 68: 284-96.
2. Lheureux S, Gourley C, Vergote I, Oza AM. Epithelial ovarian cancer. Lancet. 2019; 393: 1240-53.
3. Siegel RL, Miller KD, Jemal A. Cancer statistics, 2020. CA Cancer J Clin. 2020; 70:7-30.
4. Schenken R. Endometriosis: pathogenesis, clinical features, and diagnosis. Available at: https://www.uptodate.com/contents/endometriosis-pathogenesis-clinical-features-and-diagnosis?sectionName=Link%20to%20cancer&topicRef=83387&anchor=H2625026494&source=see_link#H2625026494. Accessed 15 November 2018.
5. Jacobs IJ, Menon U, Ryan A, *et al*. Ovarian cancer screening and mortality in the UK Collaborative Trial of Ovarian Cancer Screening (UKCTOCS): a randomised controlled trial. Lancet. 2016; 387: 945-56.
6. National Cancer Institute. Surveillance, Epidemiology, and End Results Program. Cancer stat facts: ovarian cancer. Available at: https://seer.cancer.gov/statfacts/html/ ovary.html. Accessed 30 December 2018.
7. Sisay M, Edessa D. PARP inhibitors as potential therapeutic agents for various cancers: focus on niraparib and its first global approval for maintenance therapy of gynecologic cancers. Gynecol Oncol Res Pract. 2017; 4: 18.
8. Ledermann J, Harter P, Gourley C, *et al*. Olaparib maintenance therapy in platinum-sensitive relapsed ovarian cancer. N Engl J Med. 2012; 366: 1382-92.
9. Mirza MR, Monk BJ, Herrstedt J, *et al*; ENGOT-OV16/NOVA Investigators. Niraparib Maintenance Therapy in Platinum-Sensitive, Recurrent Ovarian Cancer. N Engl J Med. 2016; 375: 2154-64.
10. Lord CJ, Ashworth A. PARP inhibitors: Synthetic lethality in the clinic. Science. 2017; 355: 1152-58.

11. Walsh CS. Two decades beyond BRCA1/2: Homologous recombination, hereditary cancer risk and a target for ovarian cancer therapy. Gynecol Oncol. 2015; 137: 343-50.
12. Lord CJ, Tutt AN, Ashworth A. Synthetic lethality and cancer therapy: lessons learned from the development of PARP inhibitors. Annu Rev Med. 2015;66:455-70.
13. Waymack PP, DeBuysere MS, Olson MS. Studies on the activation and inactivation of the branched chain alpha-keto acid dehydrogenase in the perfused rat heart. J Biol Chem. 1980; 255: 9773-81.
14. Machius M, Chuang JL, Wynn RM, *et al*. Machius M, Chuang JL, Wynn RM, Tomchick DR, Chuang DT. Structure of rat BCKD kinase: nucleotide-induced domain communication in a mitochondrial protein kinase. Proc Natl Acad Sci U S A. 2001; 98: 11218-23.
15. Jeoung NH. Pyruvate Dehydrogenase Kinases: Therapeutic Targets for Diabetes and Cancers. Diabetes Metab J. 2015;39:188-97.
16. Dupuy F, Tabariès S, Andrzejewski S, *et al*. PDK1-Dependent Metabolic Reprogramming Dictates Metastatic Potential in Breast Cancer. Cell Metab. 2015; 22: 577-89.
17. Hsu JY, Chang JY, Chang KY, *et al*. Epidermal growth factor-induced pyruvate dehydrogenase kinase 1 expression enhances head and neck squamous cell carcinoma metastasis viaup-regulation of fibronectin. FASEB J. 2017; 31: 4265-76.
18. Sun Y, Daemen A, Hatzivassiliou G, *et al*. Metabolic and transcriptional profiling reveals pyruvate dehydrogenase kinase 4 as a mediator of epithelial-mesenchymal transition and drug resistance in tumor cells. Cancer Metab. 2014; 2: 20.
19. Sun S, Liu J, Zhao M, *et al*. Loss of the novel mitochondrial protein FAM210B promotes metastasis via PDK4-dependent metabolic reprogramming. Cell Death Dis. 2017; 8: e2870.
20. McConnell BB, Burkholder B, Danner DJ. Two new mutations in the human E1 beta subunit of branched chain alpha-ketoacid dehydrogenase associated with maple syrup urine disease. Biochim Biophys Acta. 1997; 1361: 263-71.
21. Bravo-Alonso I, Oyarzabal A, Sánchez-Aragó M, *et al*. Dataset reporting BCKDK interference in a BCAA-catabolism restricted environment. Data Brief. 2016; 7: 755-9.
22. Oyarzabal A, Bravo-Alonso I, Sánchez-Aragó M, *et al*. Mitochondrial response to the BCKDK-deficiency: Some clues to understand the positive dietary response in this form of autism. Biochim Biophys Acta. 2016; 1862: 592-600.
23. Zhang D, Li N, Xi Y, *et al*. Diabetes mellitus and risk of ovarian cancer. A systematic review and meta-analysis of 15 cohort studies. Diabetes Res Clin Pract. 2017; 130: 43-52.
24. Mayers JR, Wu C, Clish CB, *et al*. Elevation of circulating branched-chain amino acids is an early event in human pancreatic adenocarcinoma development. Nat Med. 2014; 20: 1193-98.
25. Lynch CJ, Halle B, Fujii H, *et al*. Potential role of leucine metabolism in the leucine-signaling pathway involving mTOR. Am J Physiol Endocrinol Metab. 2003; 285: E854-E863.
26. Nieman KM, Kenny HA, Penicka CV, *et al*. Adipocytes promote ovarian cancer metastasis and provide energy for rapid tumor growth. Nat Med. 2011; 17:1498-503.
27. Xue P, Zeng F, Duan Q, *et al*. BCKDK of BCAA Catabolism Cross-talking With the MAPK Pathway Promotes Tumorigenesis of Colorectal Cancer. EBioMedicine. 2017; 20: 50-60.
28. Tian Q, Yuan P, Quan C, *et al*. Phosphorylation of BCKDK of BCAA catabolism at Y246 by Src promotes metastasis of colorectal cancer. Oncogene. 2020; 39: 3980-96.

29. Zhai M, Yang Z, Zhang C, *et al*. APN-mediated phosphorylation of BCKDK promotes hepatocellular carcinoma metastasis and proliferation via the ERK signaling pathway. Cell Death Dis. 2020; 11: 396.
30. Chen X, Wei S, Ma Y, *et al*. Quantitative proteomics analysis identifies mitochondria as therapeutic targets of multidrug-resistance in ovarian cancer. Theranostics. 2014; 4: 1164-75.
31. Abed MN, Richardson A. Inhibition of BCKDK increases the sensitivity of ovarian cancer cells to paclitaxel. European Journal of Cancer, 2016, 69: S20
32. Moffat J, Grueneberg DA, Yang X, *et al*. A lentiviral RNAi library for human and mouse genes applied to an arrayed viral high-content screen. Cell. 2006; 124:1283-98.
33. Hunter T, Karin M. The regulation of transcription by phosphorylation. Cell. 1992; 70: 375-87.
34. Turkoglu O, Zeb A, Graham S, *et al*. Metabolomics of biomarker discovery in ovarian cancer: a systematic review of the current literature. Metabolomics. 2016; 12: 60.
35. Fan L, Yin M, Ke C, *et al*. Use of Plasma Metabolomics to Identify Diagnostic Biomarkers for Early Stage Epithelial Ovarian Cancer. J Cancer. 2016; 7: 1265-1272.
36. Lheureux S, Gourley C, Vergote I, *et al*. Epithelial ovarian cancer. Lancet. 2019;393: 1240-53.
37. Stewart C, Ralyea C, Lockwood S. Ovarian Cancer: An Integrated Review. Semin Oncol Nurs. 2019; 35:151-6.
38. Vargas AN. Natural history of ovarian cancer. Ecancermedicalscience. 2014; 8: 465.
39. Klupczynska A, Dereziński P, Dyszkiewicz W, *et al*. Evaluation of serum amino acid profiles' utility in non-small cell lung cancer detection in Polish population. Lung Cancer. 2016; 100: 71-6.
40. Miyagi Y, Higashiyama M, Gochi A, *et al*. Plasma free amino acid profiling of five types of cancer patients and its application for early detection. PLoS One. 2011; 6: e24143.
41. Hasim A, Aili A, Maimaiti A, *et al*. Plasma-free amino acid profiling of cervical cancer and cervical intraepithelial neoplasia patients and its application for early detection. Mol Biol Rep. 2013; 40: 5853-9.
42. Gu Y, Chen T, Fu S, *et al*. Perioperative dynamics and significance of amino acid profiles in patients with cancer. J Transl Med. 2015; 13: 35.
43. Bachmayr-Heyda A, Aust S, Auer K, *et al*. Integrative Systemic and Local Metabolomics with Impact on Survival in High-Grade Serous Ovarian Cancer. Clin Cancer Res. 2017; 23: 2081-92.
44. Zhou M, Guan W, Walker LD, *et al*. Rapid mass spectrometric metabolic profiling of blood sera detects ovarian cancer with high accuracy. Cancer Epidemiol Biomarkers Prev. 2010; 19: 2262-71.
45. Ke C, Hou Y, Zhang H, *et al*. Large-scale profiling of metabolic dysregulation in ovarian cancer. Int J Cancer. 2015; 136: 516-26.
46. Hilvo M, de Santiago I, Gopalacharyulu P, *et al*. Accumulated Metabolites of Hydroxybutyric Acid Serve as Diagnostic and Prognostic Biomarkers of Ovarian High-Grade Serous Carcinomas. Cancer Res. 2016; 76: 796-804.
47. Suzuki Y, Tokinaga-Uchiyama A, Mizushima T, *et al*. Normalization of abnormal plasma amino acid profile-based indexes in patients with gynecological malignant tumors after curative treatment. BMC Cancer. 2018; 18: 973.
48. Ericksen RE, Lim SL, McDonnell E, *et al*. Loss of BCAA Catabolism during Carcinogenesis Enhances mTORC1 Activity and Promotes Tumor Development and Progression. Cell Metab. 2019; 29: 1151-65.
49. Shao D, Villet O, Zhang Z, *et al*. Glucose promotes cell growth by suppressing branched-chain amino acid degradation. Nat Commun. 2018; 9: 2935.

50. Ananieva EA, Wilkinson AC. Branched-chain amino acid metabolism in cancer. Curr Opin Clin Nutr Metab Care. 2018; 21: 64–70
51. Raffel S, Falcone M, Kneisel N, *et al*. BCAT1 restricts αKG levels in AML stem cells leading to IDHmut-like DNA hypermethylation. Nature. 2017; 551: 384-8.
52. Zheng YH, Hu WJ, Chen BC, *et al*. BCAT1, a key prognostic predictor of hepatocellular carcinoma, promotes cell proliferation and induces chemoresistance to cisplatin. Liver Int. 2016; 36: 1836-47.
53. Li JT, Yin M, Wang D, *et al*. BCAT2-mediated BCAA catabolism is critical for development of pancreatic ductal adenocarcinoma. Nat Cell Biol. 2020; 22: 167-74.
54. Suh EH, Hackett EP, Wynn RM, *et al*. In vivo assessment of increased oxidation of branched-chain amino acids in glioblastoma. Sci Rep. 2019; 9: 340.
55. Ananieva EA, Wilkinson AC. Branched-chain amino acid metabolism in cancer. Curr Opin Clin Nutr Metab Care. 2018; 21: 64-70.
56. White PJ, McGarrah RW, Grimsrud PA, *et al*. The BCKDH Kinase and Phosphatase Integrate BCAA and Lipid Metabolism via Regulation of ATP-Citrate Lyase. Cell Metab. 2018; 27: 1281-93.
57. Lian K, Du C, Liu Y, *et al*. Impaired adiponectin signaling contributes to disturbed catabolism of branched-chain amino acids in diabetic mice. Diabetes. 2015; 64: 49-59.
58. Popov KM, Hawes JW, Harris RA. Mitochondrial alpha-ketoacid dehydrogenase kinases: a new family of protein kinases. Adv Second Messenger Phosphoprotein Res. 1997; 31: 105-11.
59. Han Y, Kim B, Cho U, *et al*. Mitochondrial fission causes cisplatin resistance under hypoxic conditions via ROS in ovarian cancer cells. Oncogene. 2019; 38: 7089-105.
60. Navarro P, Bueno MJ, Zagorac I, *et al*. Targeting Tumor Mitochondrial Metabo- lism Overcomes Resistance to Antiangiogenics. Cell Rep. 2016; 15: 2705-18.

Figures

a

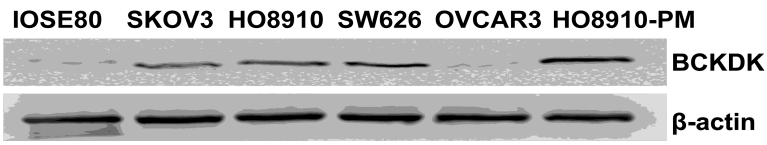

b

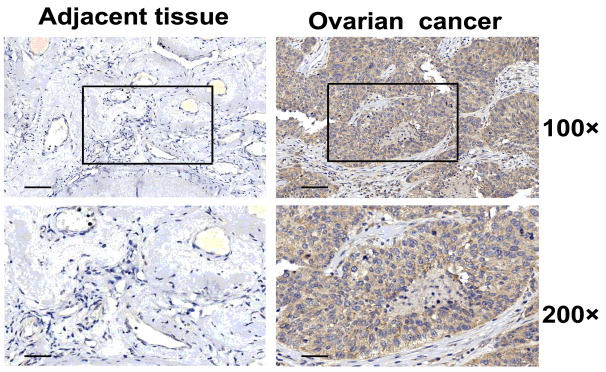

c

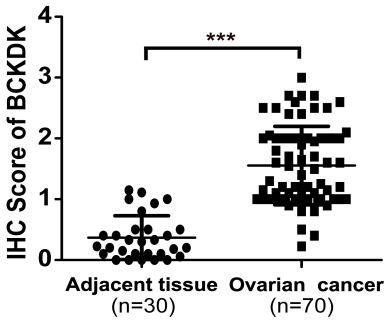

d

Clinical characteristics of 70 patients with ovarian cancer

		Grade			pT Stage		
Characteristics	Total	1	2	3	Ⅰ	Ⅱ	Ⅲ
Gender							
Male, n	0	0	0	0	0	0	0
Female, n	70	5	24	36	50	5	15
Gender ratio, M/F	0	0	0	0	0	0	0
Age, years							
Median	47.69	43.80	47.12	49	48	50.67	45.50
Range	10~84	23~54	24~67	21~75	10~84	23~66	23~62

e

	BCKDK expession		P value
	+	-	
Age			0.403
>=40	18	30	
<40	6	16	
Gender			<0.001
Male	0	0	
Female	24	46	
Grade			0.023
1	1	4	
2	4	20	
3	18	18	
pT stage			0.715
Ⅰ	17	33	
Ⅱ	1	4	
Ⅲ	6	9	
Lymph node metasis			0.094
yes	0	5	
no	24	41	

Figure 1

BCKDK overexpression is associated with advanced pathological grade in EOC patients. (a) Expression of BCKDK in 6 different ovarian cell lines. (b) Immunohistochemical examination for the expression of BCKDK in 70 cases of human epithelial ovarian cancer tissues and 30 of adjacent tissues. Pictures from 1 representative case are shown in the upper panel, and the 2 scale bars from up to down in each group correspond to 100 and 40 μm respectively. (c) Statistics of the IHC examination results are shown. The IHC score of BCKDK is higher in EOC tissues than adjacent tissues. (d) The clinical characteristics of 70 patients with ovarian cancer. (e) The correlation between BCKDK expression and clinicopathologic features, Correlation data were determined by using Pearson correlation coefficients. Error bars represent the mean ± SD values. (***, $P < 0.001$).

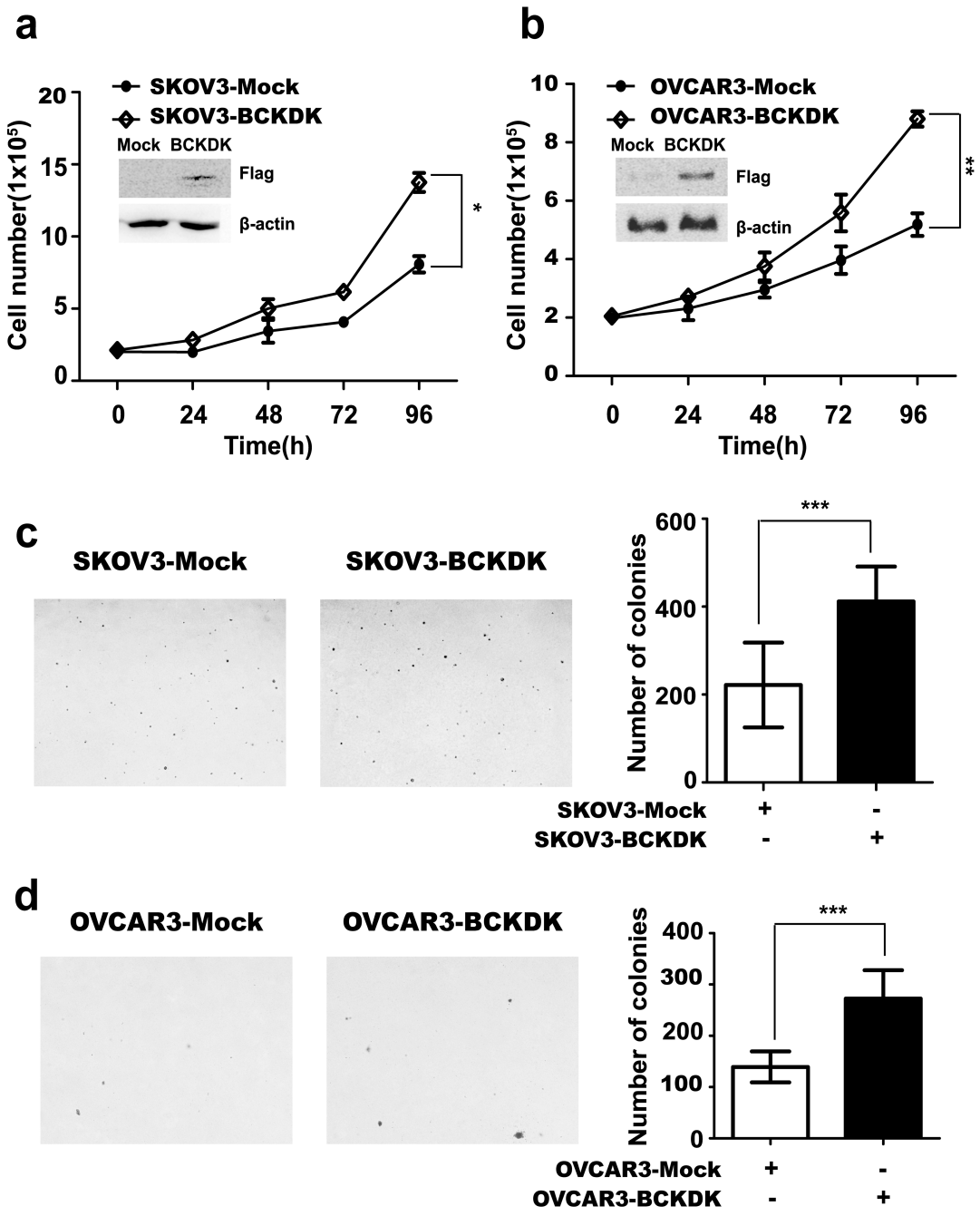

Figure 2

BCKDK promotes EOC cell proliferation. (a) Growth curves of vector control cells (SKOV3-Mock) and BCKDK-overexpressing cells (SKOV3-BCKDK). Insert shows verification of the cell lines identified by Western blot. Data are represented as mean ± standard deviation from triplicate experiments. The asterisk indicates a significant increase in cell number in SKOV3-BCKDK cells compared with SKOV3-Mock cells (*, P<0.05). (b) Growth curves of vector control cells (OVCAR3-Mock) and BCKDK-overexpressing cells (OVCAR3-BCKDK). Insert shows verification of the cell lines identified by Western blot. Data are represented as mean ± standard deviation from triplicate experiments. The asterisk indicates a significant increase in cell number in OVCAR3-BCKDK cells compared with OVCAR3-Mock cells (**, P<0.01). (c) BCKDK can transform SKOV3 cells ex vivo as illustrated by growth of BCKDK transformed cells in soft agar. Photomicrograph of representative colony formation in soft agar of vector control cells (SKOV3-

Mock) compared with BCKDK-overexpression cells (SKOV3-BCKDK) is shown (***, P<0.001). (d) BCKDK can enhance the transformation of OVCAR3 cells ex vivo as illustrated by growth of BCKDK transformed cells in soft agar. Photomicrograph of representative colony formation in soft agar of vector control cells (OVCAR3-Mock) compared with BCKDK-overexpressing cells (OVCAR3-BCKDK) is shown (***, P<0.001).

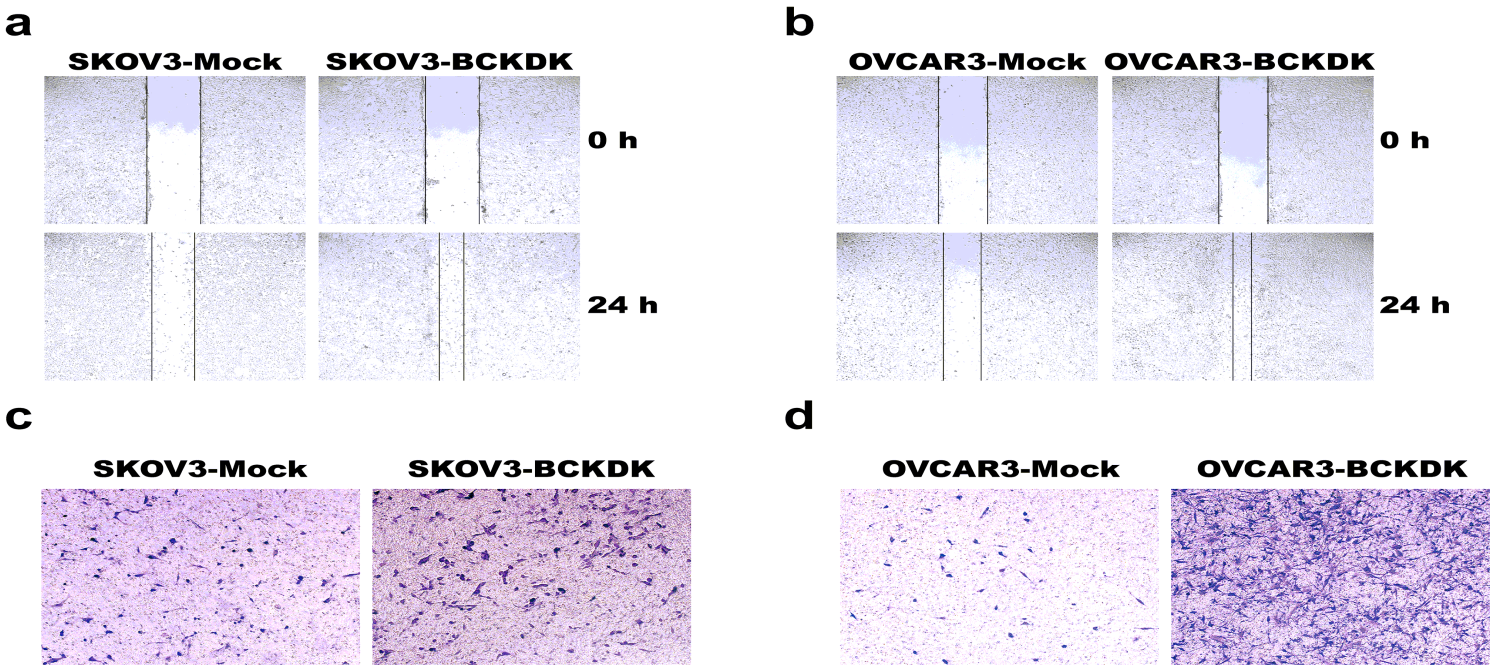

Figure 3

BCKDK promotes EOC cell migration. (a) Scratch wound assay demonstrating that SKOV3-Mock migrate faster thanSKOV3-BCKDK cells. The dotted lines show the area where the scratch wound was created. The scratch wound assay was performed in triplicate experiments. (b) Scratch wound assay demonstrating that OVCAR3-Mock migrate faster thanOVCAR3-BCKDK cells. The dotted lines show the area where the scratch wound was created. The scratch wound assay was performed in triplicate experiments.(c) Transwell invasion assay. SKOV3-BCKDK have greater invasive capacity than SKOV3-Mock cells. Representative images from Transwell invasion assays of SKOV3-Mock cells and SKOV3-BCKDK cells are shown. (d) Transwell invasion assay. OVCAR3-BCKDK have greater invasive capacity than OVCAR3-Mock cells. Representative images from Transwell invasion assays of OVCAR3-Mock cells and OVCAR3-BCKDK cells are shown.

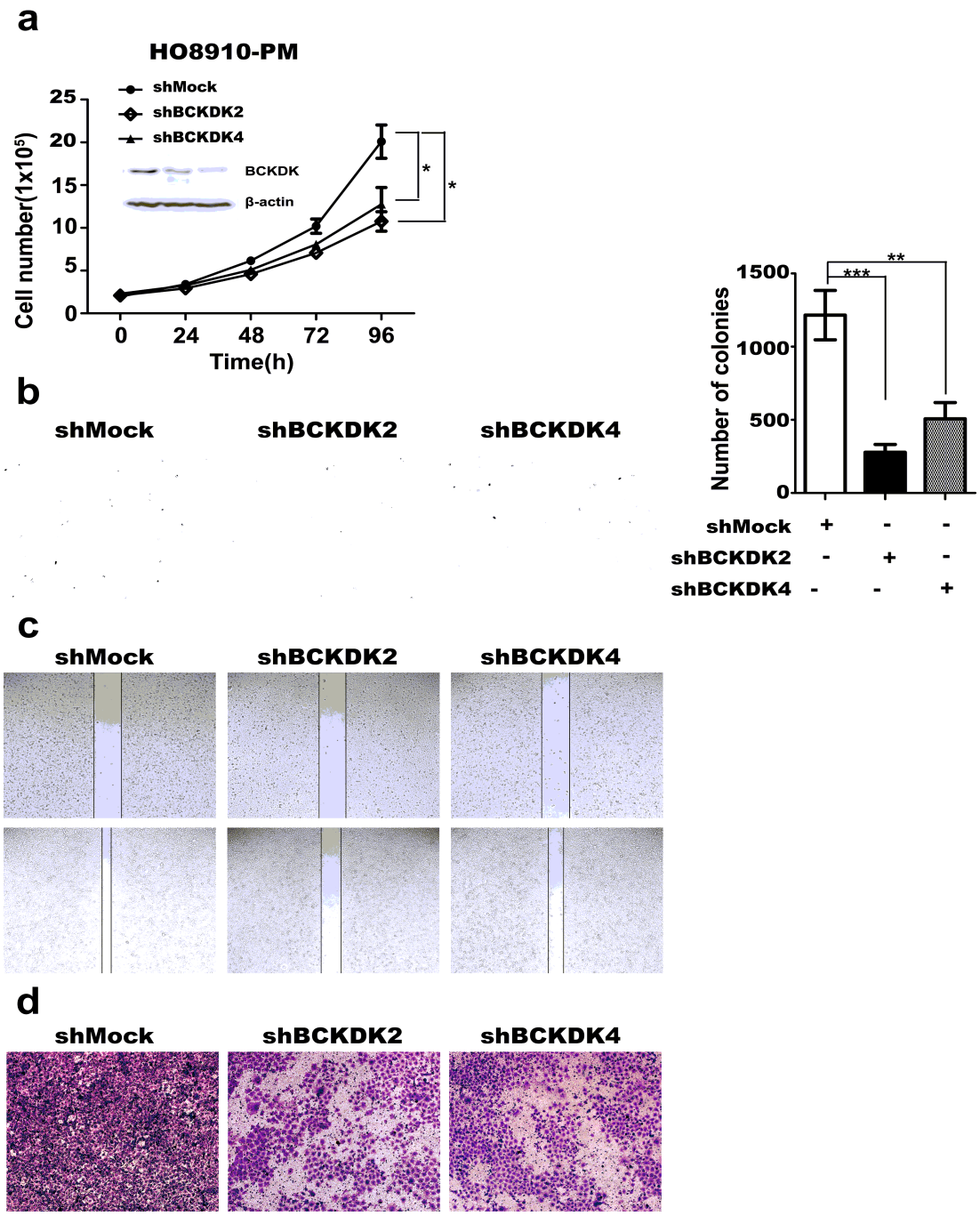

Figure 4

Knockdown of BCKDK attenuates EOC tumor properties ex vivo. (a) Growth curves of HO8910-PM-shMock, HO8910-PM-shBCKDK2, and HO8910-PM-shBCKDK4 cells. Insert shows verification of the knockdown cell lines identification by Western blot. Data are represented as mean ± standard deviation from triplicate experiments. The asterisks indicate a significant increase compared with shMock cells (*, P<0.05). (b) Knockdown of BCKDK reduces tumorigenic properties of HO8910-PM cells ex vivo. Representative photomicrograph of colony formation in soft agar of vector control cells (shMock) compared with BCKDK-knockdown cells (shBCKDK2 or shBCKDK4) is shown. Data are represented as mean ± standard eviation from triplicate experiments (**, P<0.01; ***, P<0.001). (c) Scratch wound assay demonstrating that HO8910-PM-shMock migrate faster than HO8910-PM-shBCKDK2, 4 cells. The dotted lines show the area where the scratch wound was created. The scratch wound assay was performed in

triplicate experiments.(d) Transwell invasion assay. HO8910-PM-shMock have greater invasive capacity than HO8910-PM-shBCKDK2, 4 cells. Representative images from Transwell invasion assays of HO8910-PM-shMock cells and HO8910-PM-shBCKDK2, 4 cells are shown.

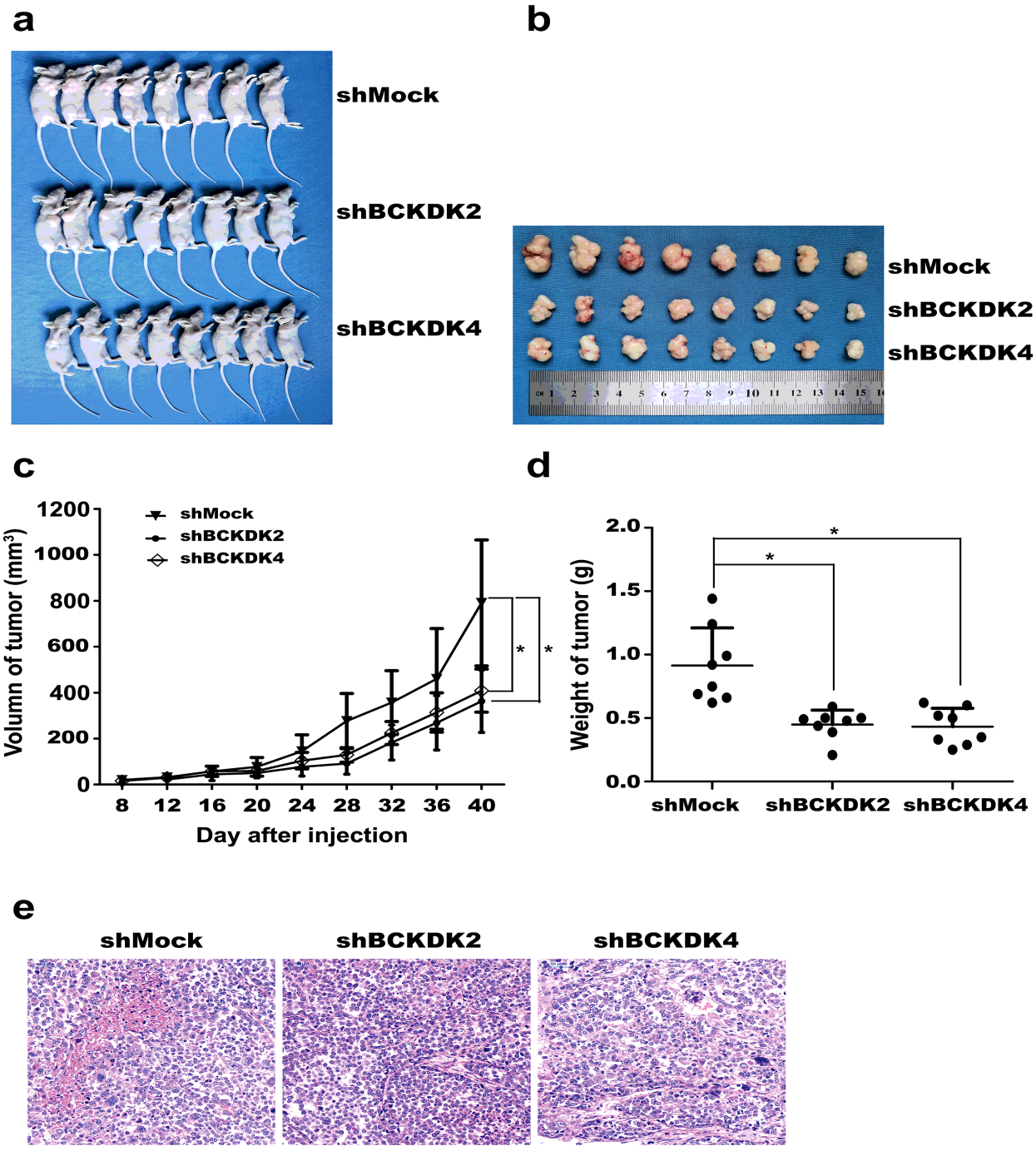

Figure 5

Knockdown of BCKDK reduces tumorigenic properties of HO8910-PM cells in vivo. (a) Mice and (b) tumors dissected from each group are shown. (c) Final average tumor growth curve and (d) tumor weight of mice injected with HO8910-PM-shMock or HO8910-PM-shBCKDK cells is shown. Data are shown as means ± standard deviation of measurements. The asterisk indicates a signifificant decrease in tumor size of HO8910-PM-shBCKDK-injected mice compared with HO8910-PM-shMock-injected mice (*, P<0.05). (e) Immunohistochemistry analysis was performed in the tumor tissues of HO8910-PM-shMock-injected mice or HO8910-PM-shBCKDK-injected mice.

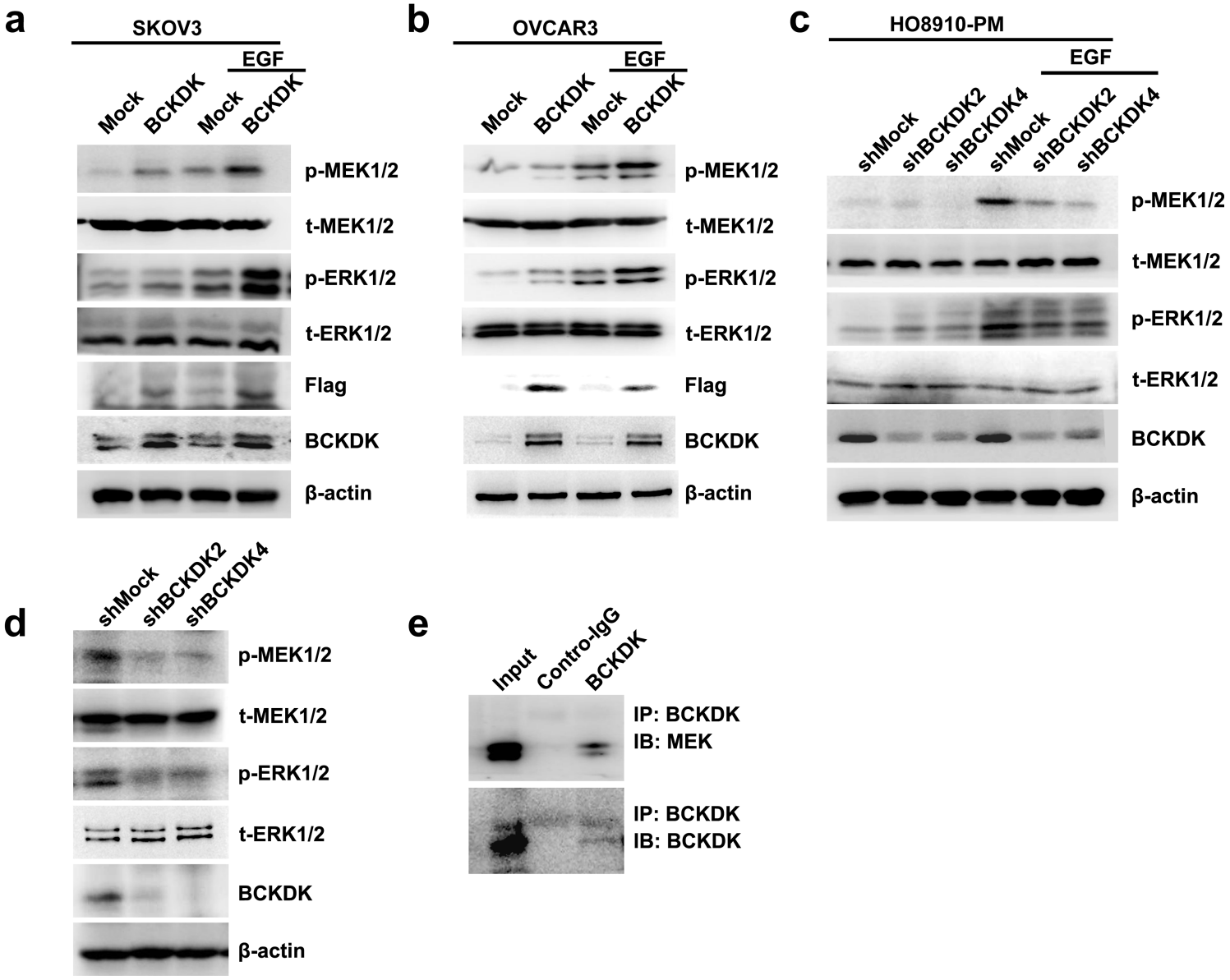

Figure 6

BCKDK promotes tumorigenesis through up-regulating MEK-ERK signaling pathway. (a, b) The level of phosphorylation of MEKs and ERKs were increased in SKOV3/OVCAR3-BCKDK cells after EGF treatment for 15 min. (c) The level of phosphorylation of MEKs and ERKs were decreased in HO8910-PM-shBCKDK cells after EGF treatment for 15 min. (d) The level of phosphorylation of MEKs and ERKs were decreased in the tumor tissues from HO8910-PM-shBCKDK-injected mice compared to HO8910-PM-shMock-injected mice. (e) BCKDK binds with MEK in HO8910-PM cells. Endogenous BCKDK was immunoprecipitated from HO8910-PM cells and then probed with anti-MEK antibody. All Western blot data are representatives of results from triplicate experiments.

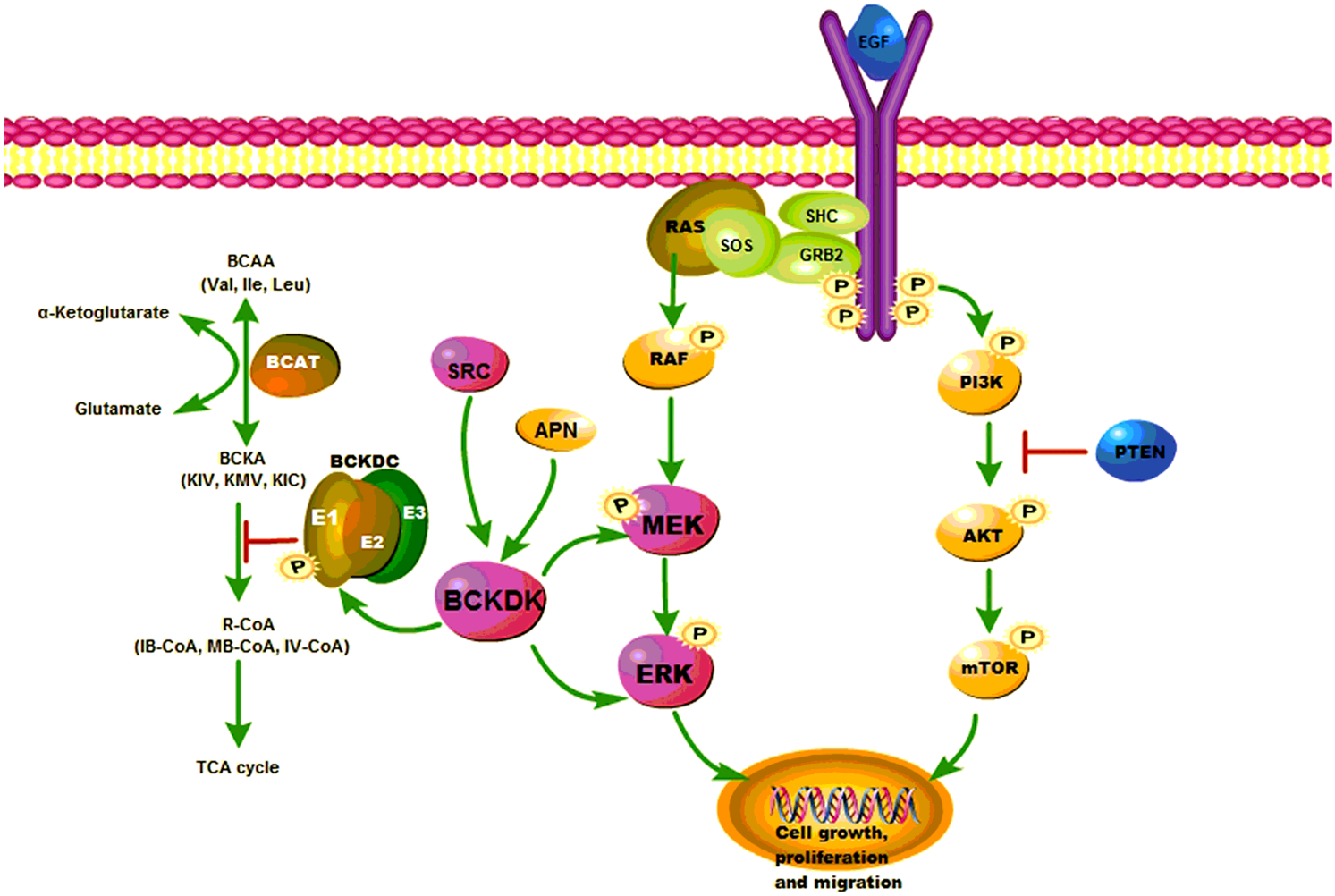

Figure 7

The signaling pathway of BCKDK in cancers 27-29.